

A new boron cluster anion pillared metal organic framework with ligand inclusion and its selective acetylene capture properties

Wanqi Sun,^{a§} Yujie Jin,^{b§} Yilian Wu,^a Wushuang Lou,^a Yanbin Yuan,^a Simon Duttwyler,^b Lingyao Wang,^a Yuanbin Zhang^{a*}

a Key Laboratory of the Ministry of Education for Advanced Catalysis Materials, College of Chemistry and Life Sciences, Zhejiang Normal University, Jinhua 321004, China. E-mail: ybzhang@zjnu.edu.cn

b Department of Chemistry, Zhejiang University 38 Zheda Road, 310027 Hangzhou, P. R. China

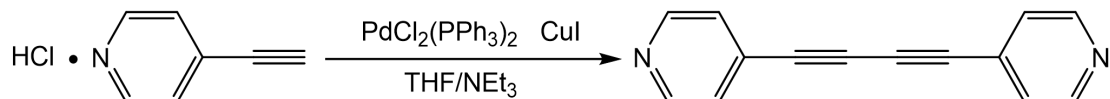
[§] These authors contributed equally to this work.

General Information and Procedures

Unless otherwise noted, all the reactions were performed under air without N₂ or Ar protection. All reagents were used as received without purification unless stated otherwise.

Chemicals: The basic starting material Na₂[B₁₂H₁₂]·2H₂O was purchased from Yuanli Technology Company. Cu[NO₃]₂·3H₂O was purchased from Aladdin. 4-Ethynylpyridine hydrochloride, bis(triphenylphosphine) palladium(II) chloride and copper(I) Iodide was purchased from Energy Chemical. C₂H₂ (99.5%), C₂H₄ (99.9%), CO₂ (99.9%), C₂H₂/CO₂ (50:50) and C₂H₂/C₂H₄ (1:99) were purchased from Datong Co., Ltd. (Jinhua). All other reagents were purchased from Adamas-beta and used without further purification.

Preparation of 1,4-di(pyridin-4-yl)buta-1,3-diyne (L6):



Scheme S1. Synthesis of 1,4-di(pyridin-4-yl)buta-1,3-diyne (L6).

Ethynylpyridine hydrochloride (1g, 7.16 mmol), CuI (0.0682g, 0.358mmol), bis(triphenylphosphine) palladium(II) chloride (0.251g, 0.358mmol) was added into a 250 ml round-bottom flask, followed by 20 mL of THF and 60 mL of NEt₃. The reaction mixture was stirred at room temperature for 12 h until TLC showed the disappearance of the starting material. Then the reaction mixture was filtered through celite, washed by THF (4 mL × 4). The filtrate was collected and concentrated under vacuum using rotatory evaporator, and purified by column chromatography (DCM: MeCN = 10:1) to give slight yellow solid. Yield: 86%.

¹H NMR (CDCl₃, 400 MHz): δ 8.64 (dd, J= 5.8 Hz, J=1.3 Hz, 4H), 7.39 (d, J= 5.8 Hz, J=1.3 Hz, 4H);

¹³C{¹H} NMR (CDCl₃, 101 MHz): 149.8 (CH), 129.6 (C_{quat}), 126.2 (CH), 80.3 (C_{quat}), 77.3 (C_{quat})

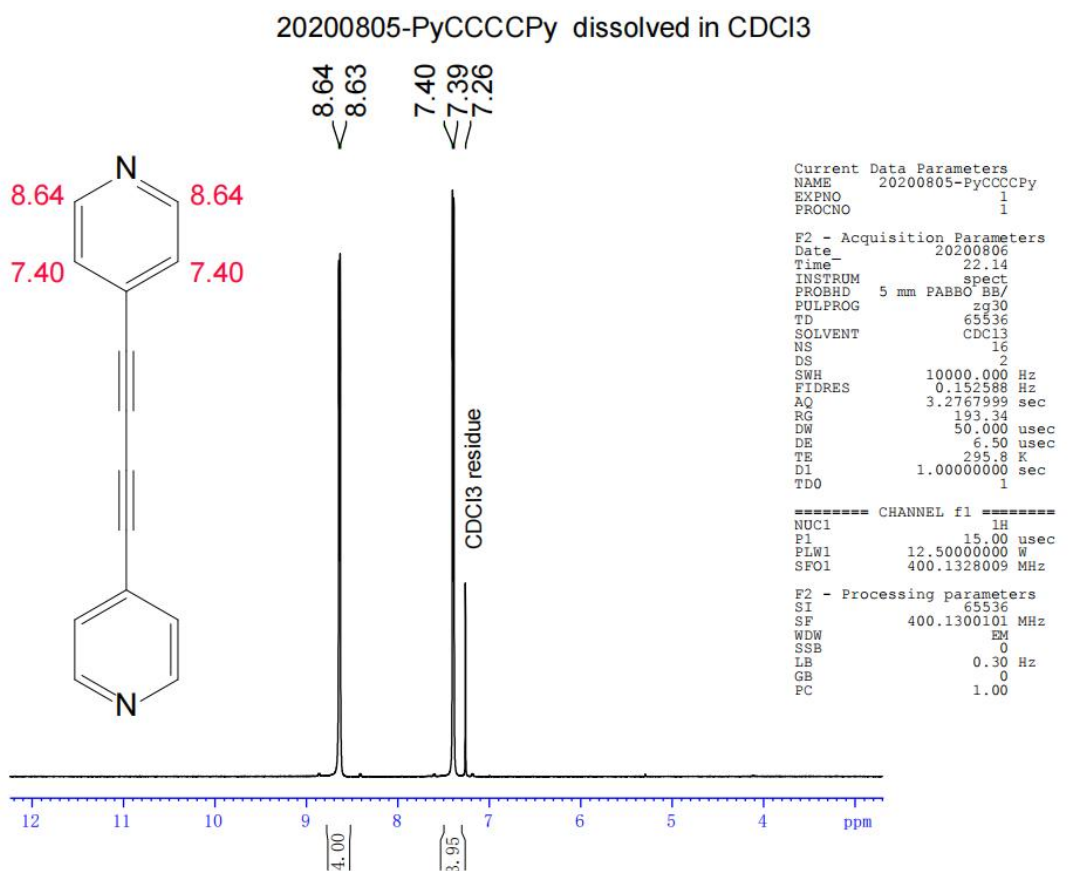


Fig. S1 ¹H NMR spectrum of L6.

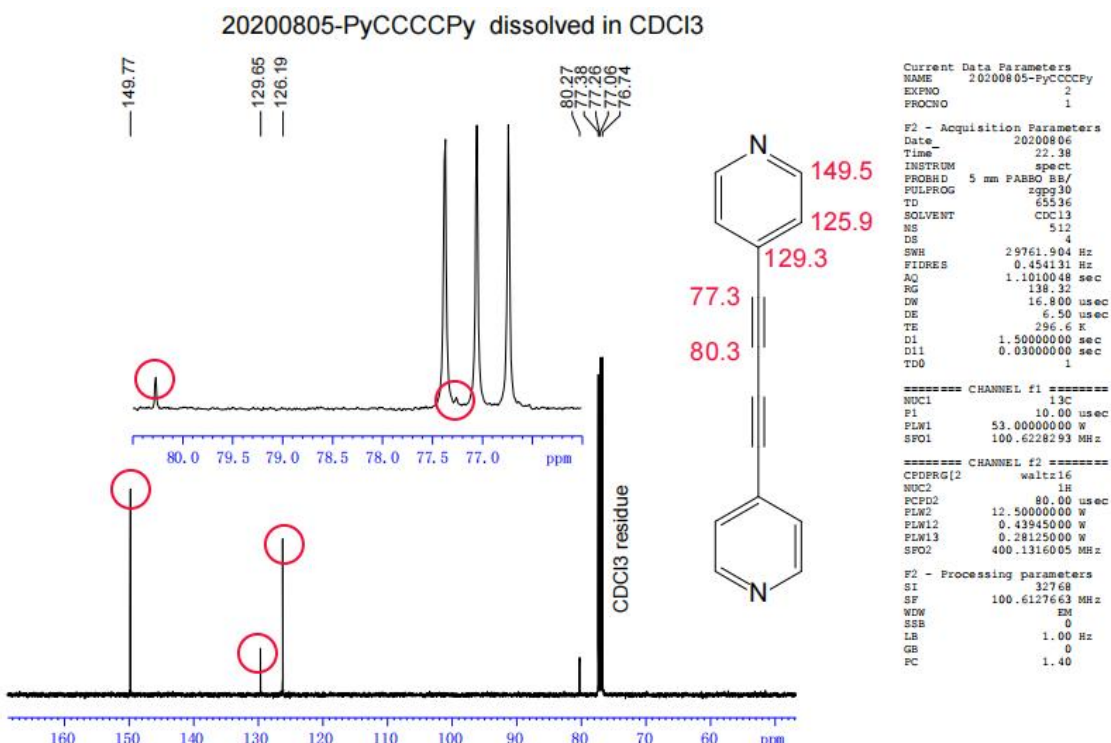


Fig. S2 ¹³C{¹H} NMR spectrum of L6.

Preparation of single crystals of BSF-10: To a 4 mL long thin tube was added a 1 mL of aqueous solution with $[\text{Na}]_2[\text{B}_{12}\text{H}_{12}]\cdot 2\text{H}_2\text{O}$ (~ 1 mg) and $\text{Cu}[\text{NO}_3]_2\cdot 3\text{H}_2\text{O}$ (~ 1 mg). 1 mL of MeOH/H₂O mixture and 2 mL MeOH was slowly layered above the solution, followed by a 1 mL of MeOH solution of 1,4-di(pyridin-4-yl)buta-1,3-diyne (2 mg). The tube was sealed and left undisturbed at 298 K. After ~ 1 week, dark brown single crystals suitable for X-ray diffraction analysis were obtained. Changing the ratio of $\text{Cu}[\text{B}_{12}\text{H}_{12}]:\text{L6}$ has no influence on the crystal structure indicated by the X-ray structural analysis. Yield: 60.5%.

Bulky synthesis of BSF-10: A mixture of $[\text{Na}]_2[\text{B}_{12}\text{H}_{12}]\cdot 2\text{H}_2\text{O}$ (120 mg, 0.54 mmol) and $\text{Cu}[\text{NO}_3]_2\cdot 3\text{H}_2\text{O}$ (118 mg, 0.49 mmol) was dissolved in 5 mL of MeOH in a 50 mL round bottom flask and heated to 35 °C. Then a MeOH (30 mL) solution of 1,4-di(pyridin-4-yl)buta-1,3-diyne (200 mg, 1 mmol) was slowly added to the above solution during string (500 rpm), dark brown solid formed immediately, and the suspension was stirred at 35 °C for another 48 h. The solid was then collected by filtration, washed by MeOH (10 mL), and soaked in anhydrous MeOH for storage. Yield: 84%.

Single-crystal X-ray diffraction studies were conducted at 296 K on the Bruker D8 VENTURE diffractometer equipped with a PHOTON-II detector ($\text{MoK}\alpha$, $\lambda = 0.71073 \text{ \AA}$).

Powder X-ray diffraction (PXRD) data were collected on a SHIMADZU XRD-6000 diffractometer ($\text{Cu K}\alpha\lambda = 1.540598 \text{ \AA}$) with an operating power of 40 KV, 30 mA and a scan speed of 4.0°/min. The range of 2θ was from 5° to 50°.

Thermal gravimetric analysis was performed on a TGA Q500 V20.13 Build 39 instrument. Experiments were carried out using a platinum pan under nitrogen atmosphere which conducted by a flow rate of 60 mL/min nitrogen gas. The data were collected at the temperature range of 50 °C to 800 °C with a ramp of 10 °C /min.

The gas adsorption measurements were performed on a Builder SSA 7000 instrument (Beijing Builder Electronic Technology, Co., Ltd). Before gas adsorption measurements, the sample of BSF-10 was evacuated at 25° C for 2 hours firstly, and then at 75° C for 12 h. The adsorption isotherms were collected at 278 and 298 K on activated samples. The experimental temperatures were controlled by liquid nitrogen bath (77 K) and water bath (278, 298 K), respectively.

Fitting of experimental data on pure component isotherms

The unary isotherms for C₂H₂, CO₂ and C₂H₄, measured at two different temperatures 278 K, and 298 K in BSF-10 were fitted with excellent accuracy using the dual-site Langmuir-Freundlich model. For dual-site Langmuir-Freundlich model, two distinct adsorption sites A and B are distinguished:

$$q = q_{A, \text{sat}} \frac{b_A p^{v_A}}{1 + b_A p^{v_A}} + q_{B, \text{sat}} \frac{b_B p^{v_B}}{1 + b_B p^{v_B}} \quad (1)$$

Here, P is the pressure of the bulk gas at equilibrium with the adsorbed phase (kPa), q is the adsorbed amount per mass of adsorbent (L kg⁻¹), q_{A,sat} and q_{B,sat} are the saturation capacities of site A and B (L kg⁻¹), b_A and b_B are the affinity coefficients of site A and B (kPa^{-v}), and v_A and v_B represent the deviations from an ideal homogeneous surface.

The binding energy is reflected in the isosteric heat of adsorption, Q_{st}, defined as:

$$Q_{st} = RT^2 \left(\frac{\partial \ln p}{\partial T} \right)_q \quad (2)$$

The calculations are based on the use of the Clausius-Clapeyron equation.

IAST calculations of adsorption selectivity

The IAST adsorption selectivity for two gases is defined as:

$$S_{ads} = \frac{q_1/q_2}{p_1/p_2} \quad (3)$$

q₁, and q₂ are the molar loadings in the adsorbed phase in equilibrium with the bulk gas phase with partial pressures p₁, and p₂.

Breakthrough experiments

The breakthrough experiments were carried out on a dynamic gas breakthrough equipment HPMC-41 (Xuzhou North Gaorui Electronic Equipment Co., Ltd). The experiments were conducted using a stainless steel column (4.6 mm inner diameter × 50 mm length). The weight of BSF-10 powder packed in the columns were 0.233 g. The column packed with BSF-10 was first purged with a Ar flow (5 mL min^{-1}) for 12 h at 75°C . The mixed gas of $\text{C}_2\text{H}_2/\text{CO}_2$ (50/50, v/v) and $\text{C}_2\text{H}_2/\text{C}_2\text{H}_4$ (1/99, v/v) was then introduced. Outlet gas from the column was monitored using gas chromatography (GC-9860-5CNJ) with the thermal conductivity detector TCD. After the breakthrough experiment, the sample was regenerated with a Ar flow of 5 mL min^{-1} under 75°C for 8 h.

Calculation of separation factor (α)

The amount of gas adsorbed i (q_i) is calculated from the breakthrough curve using the following:

$$q_i = \frac{V_T P_i \Delta T}{m} \quad (4)$$

Here, V_T is the total flow rate of gas (cm^3/min), P_i is the partial pressure of gas i (atm), ΔT is the time for initial breakthrough of gas i to occur (mins) and m is the mass of the sorbent (g). The separation factor (α) of the breakthrough experiment is determined as

$$\alpha = \frac{q_1 y_2}{q_2 y_1} \quad (5)$$

Where, y_i is the partial pressure of gas i in the gas mixture.

II Characterization of BSF-10



Fig. S3 Photography of the single crystals of BSF-10.

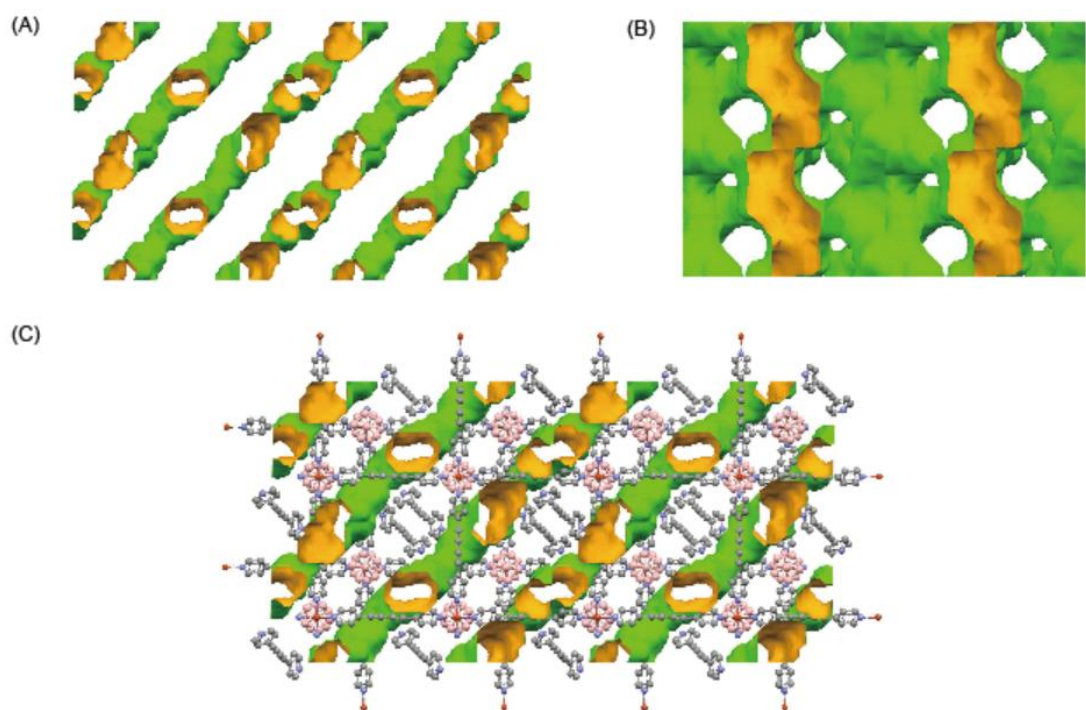
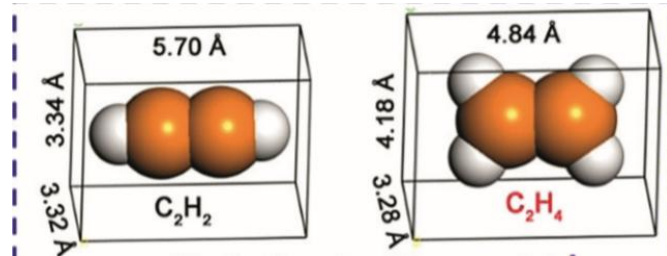


Fig. S4 Voids of BSF-10 viewed along the crystallographic b-axis (A, C) and c-axis (B).

Table S1. Comparison of C₂H₂, C₂H₄ and CO₂

Gas molecules	Kinetic Size (Å)	Molecular size (Å ³)	Boiling point (K)	Quadrupole Moment (C m ²)
C ₂ H ₂	3.3	3.32 x 3.34 x 5.70	189.3	20.5 x 10 ⁻⁴⁰
CO ₂	3.3	3.18 x 3.33 x 5.36	194.7	-13.4 x 10 ⁻⁴⁰
C ₂ H ₄	4.163	3.28 x 4.18 x 4.84	169.5	

**Table S2.** Summary of the crystallographic parameters of BSF-1, BSF-3, and BSF-10.

Materials	BSF-1	BSF-3	BSF-10
Cell	a=28.764(2)	a=19.8856(17)	a=16.1422(6)
	b=17.1839(11)	b=22.4095(18)	b=10.1054(3)
	c=19.918(3)	c=21.0263(16)	c=32.1517(11)
	α=90	α=90	α=90
	β=133.107(2)	β=90	β=90.671(1)
	γ=90	γ=90	γ=90
Temperature	173 K	193 K	296K
Volume (Å ³)	7187.6(13)	9369.9(13)	5244.3(3)
Space group	C 2/c	Ima2	P 21/c
Hall group	-C2yc	I2-2a	-P 2ybc
formula	C ₂₄ H ₂₈ B ₁₂ CuN ₄	C ₃₂ H ₃₆ B ₁₂ CuN ₄	C ₄₂ H ₃₆ B ₁₂ CuN ₆
MW	565.77	669.91	818.03
density	1.046	0.95	1.036
Z	8	8	4
R	0.0684	0.0912	0.0826 (9146)
wR2	0.1859	0.2616	0.2273 (12012)
S	1.043	1.121	1.079

Table S3. Summary of the crystallographic parameters of different Cu[B₁₂H₁₂]:L6 ratio.

Feeding	Cu[B ₁₂ H ₁₂]:L6 = 1:2	Cu[B ₁₂ H ₁₂]:L6 = 1:4
Cell	a=16.1372(17)	a=16.1422(6)
	b=10.0899(11)	b=10.1054(3)
	c=32.096(4)	c=32.1517(11)
	α =90	α =90
	β =90.883	β =90.671(1)
	γ =90	γ =90
Temperature	296 K	296 K
Volume (Å ³)	5225.3(10)	5244.3(3)
Space group	P 21/c	P 21/c
Hall group	-P 2ybc	-P 2ybc
formula	C ₄₂ H ₃₆ B ₁₂ CuN ₆	C ₄₂ H ₃₆ B ₁₂ CuN ₆
MW	818.03	818.03
density	1.040	1.036
Z	4	4
R	0.1058 (6748)	0.0826 (9146)
wR2	0.2848 (9128)	0.2273 (12012)
S	1.138	1.079

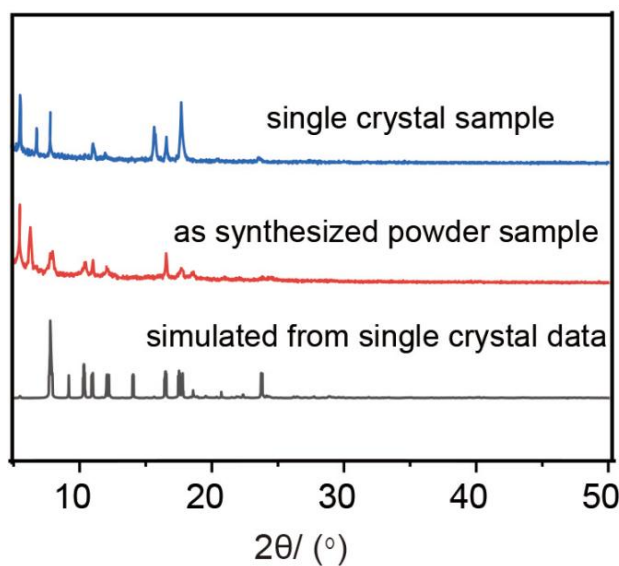


Fig. S5 PXRD patterns of BSF-10.

Explanation: The difference between the as-synthesized PXRD pattern and the one simulated from scXRD has slight difference. There are usually two reason to cause such difference: 1) the simulated PXRD is from a high quality single crystal but the PXRD measurement need bulky samples. Structural discrepancy, which is possible to avoid in real-world system may lead to slight difference. 2) the size of the sample particle as well as the grind process before measurements may also make some changes of the PXRD pattern, especially on the peak strength. The as-synthesized single crystals and powder feature nearly identical PXRD pattern, indicating the purity of bulky samples.

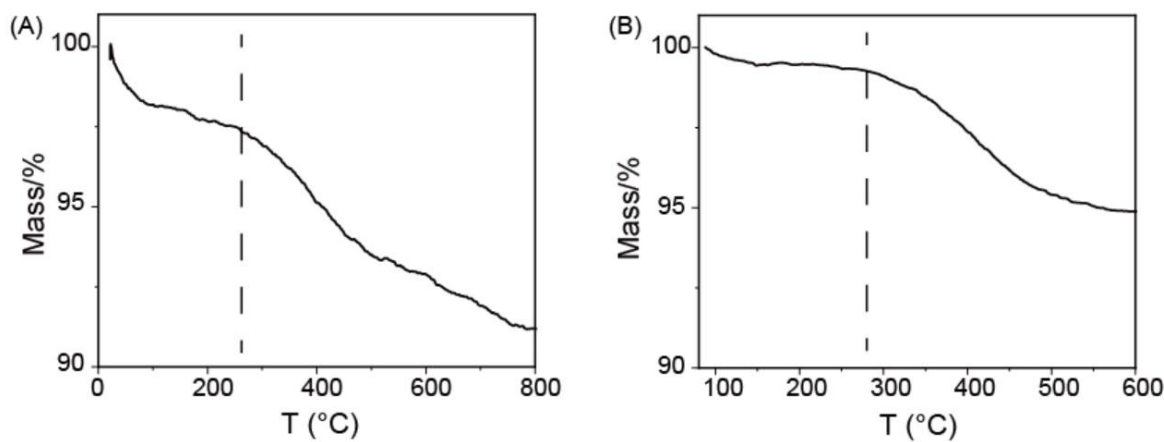


Fig. S6 TGA curves of the as-synthesized (A) and activated (B) BSF-10.

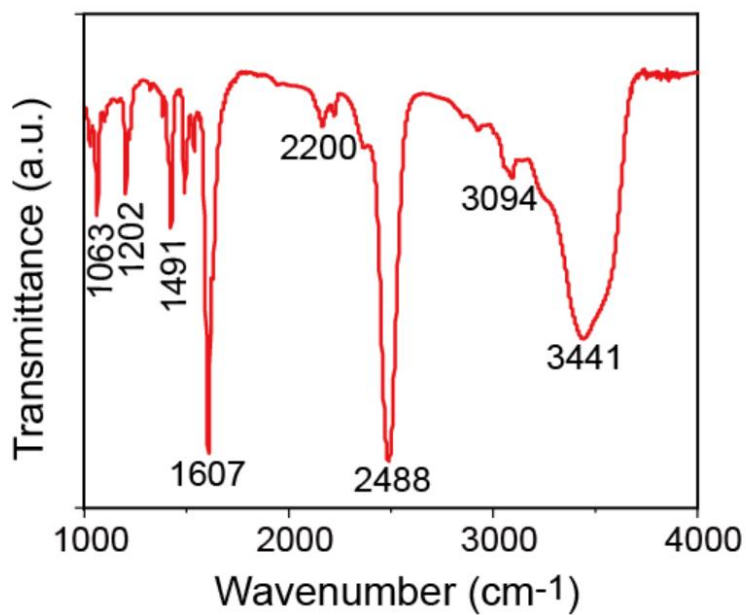


Fig. S7 Fourier transform infrared (FTIR) spectrum of BSF-10.

Analysis: The sharp peaks at 2488 cm⁻¹ is B-H stretch vibration peak. The sharp peak at 1607 cm⁻¹ is the stretch vibration peaks of the aromatic (Py) C=C and C=N. The small peaks at 3094 is C(Py)-H stretch vibration peak. The small peaks at around 2200 cm⁻¹ is C≡C stretch vibration peak.

III Adsorption data, IAST selectivity

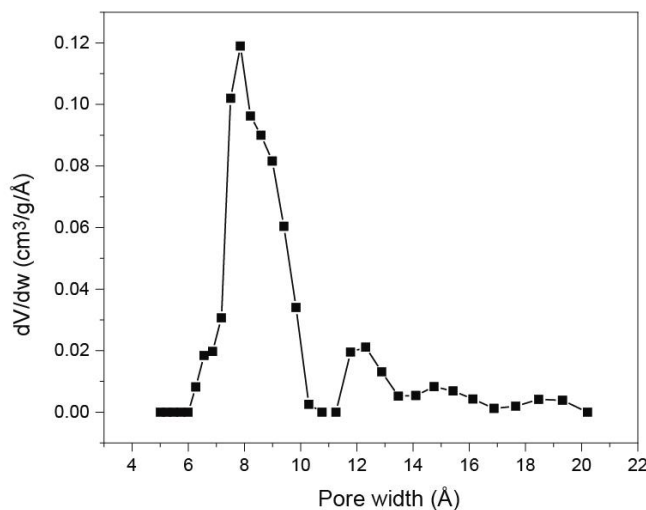


Fig. S8 Pore size distribution of BSF-10 calculated from 77 K N₂ adsorption isotherms.

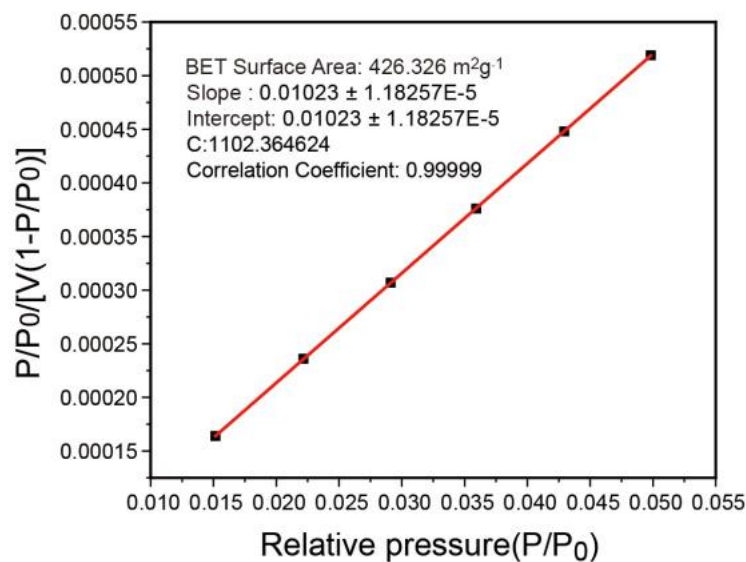


Fig. S9 BET surface area plot of BSF-10.

Table S4 Langmuir - Freundlich parameters fit for C₂H₂, C₂H₄, CO₂ in BSF-10 at 278K.

	Site A			Site B			correlation Coefficient (R ²)
	q _{A,sat} (L kg ⁻¹)	b _A (kPa ^{-vA})	v _A	q _{B,sat} (L kg ⁻¹)	b _B (kPa ^{-vB})	v _B	
C ₂ H ₂	56.39	0.000302	1.74	61.77	0.13	0.76	0.99999
C ₂ H ₄	32.83	0.00069	1.55	48.90	0.05	0.89	0.99999
CO ₂	798.04	0.00016	1.14	25.48	0.0249	0.91	0.99999

Table S5 Langmuir - Freundlich parameters fit for C₂H₂, C₂H₄, CO₂ in BSF-10 at 298 K.

	Site A			Site B			correlation Coefficient (R ²)
	q _{A,sat} (L kg ⁻¹)	b _A (kPa ^{-vA})	v _A	q _{B,sat} (L kg ⁻¹)	b _B (kPa ^{-vB})	v _B	
C ₂ H ₂	57.24	0.069	0.84	71.9	0.00014	1.72	0.99999
C ₂ H ₄	10.29	0.052	0.99	90.37	0.0077	0.91	0.99999
CO ₂	5.65	0.04	0.90	354	0.0005	1.05	0.99998

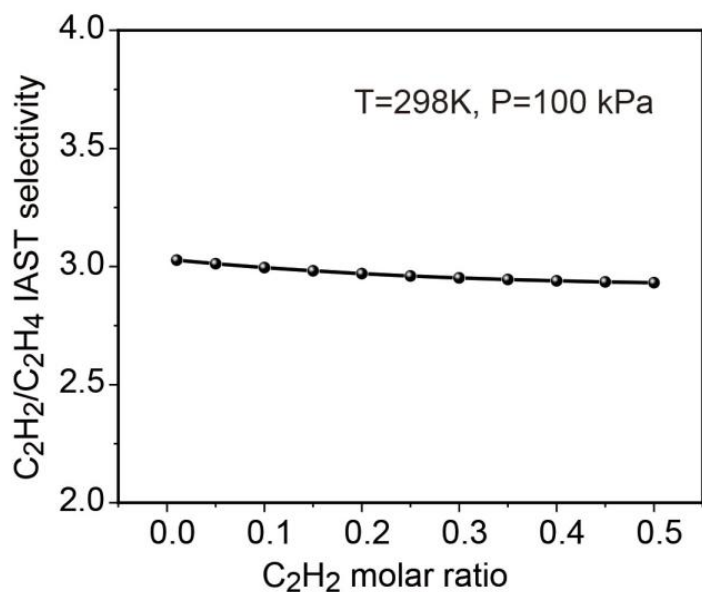


Fig. S10 IAST selectivity of BSF-10 towards a gas mixture of $\text{C}_2\text{H}_2/\text{C}_2\text{H}_4$ (50/50) at 298 K with different C_2H_2 ratio.

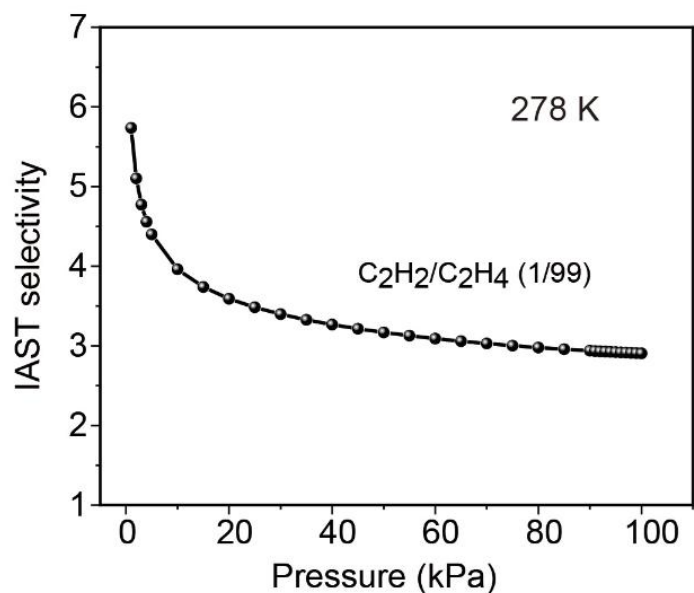


Fig. S11 IAST selectivity (5.74-2.91) of BSF-10 towards a gas mixture of $\text{C}_2\text{H}_2/\text{C}_2\text{H}_4$ (1/99) at 278.

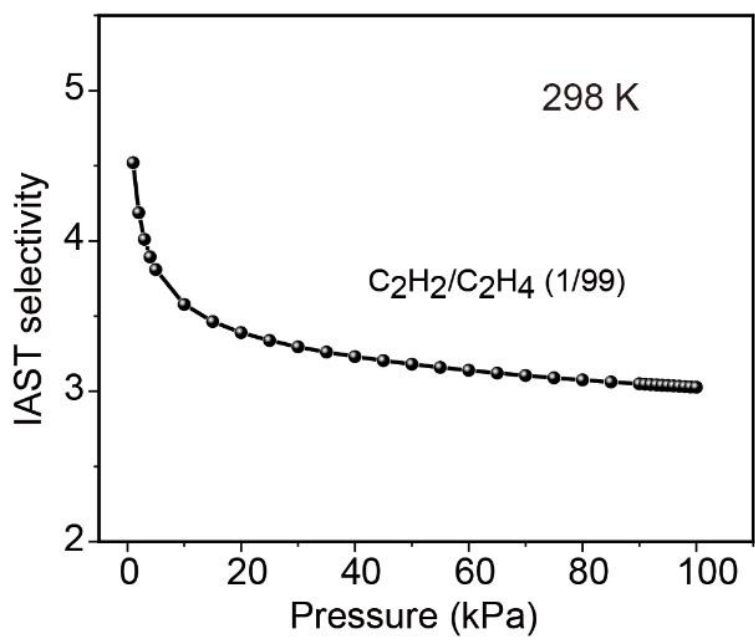


Fig. S12 IAST selectivity (4.52-3.03) of BSF-10 towards a gas mixture of C₂H₂/C₂H₄ (1/99) at 298 K.

Table S6 Summary of the gas adsorption data of BSF-1, BSF-3, BSF-10.

Materials		BSF-1	BSF-3	BSF-10
C ₂ H ₂ uptake at 298 K (mmol/g)	1 bar	2.35	3.59	2.9
CO ₂ uptake at 298 K (mmol/g)	1 bar	1.77	2.11	1.15
C ₂ H ₄ uptake at 298 K (mmol/g)	1 bar	1.63	2.37	1.76
C ₂ H ₂ /CO ₂ (1:1) IAST selectivity (298K)	1-100 kPa	4.79-3.36	16.49-16.29	13.52-5.86
C ₂ H ₂ /C ₂ H ₄ (1:1) IAST selectivity (298K)	1-100 kPa	2.3	8	4.09-2.93
C ₂ H ₂ Q_{st} (kJ/mol)		30.7	42.7	34.8
C ₂ H ₄ Q_{st} (kJ/mol)		26	22.4	27.4
CO ₂ Q_{st} (kJ/mol)		21.7	28.1	22.9
BET surface area (m ² /g)		535	458	426

Table S7 Comparison of the C₂H₂/CO₂ breakthrough separation performance of BSF-10 with other materials at room temperature.

Materials	C ₂ H ₂ uptake ^[a] (mmol/g)	Separation factor ^[b]	Ref.
BSF-10	2.0	2.8	This work
CAU-10-H	3.3	3.4	[1]
Cu ^I @UiO-66-(COOH) ₂	2.89	3.4	[2]
JCM-1	2.2	4.4	[3]
NKMOF-1-Ni	2.48	2.6	[4]
FJU-90	1.87	2.1	[5]
HOF-3a	1.12	2	[6]

[a] Adsorption uptake obtained from breakthrough experiments.

[b] Separation factor is calculated from breakthrough curves.

Table S8 Comparison of the reported materials on C₂H₂/CO₂ adsorption capacity, adsorption enthalpy (Q_{st}), IAST selectivity of C₂H₂/CO₂ and C₂H₂/CO₂ uptake ratio.

Porous Materials	C ₂ H ₂ uptake (cm ³ /g)	CO ₂ uptake (cm ³ /g)	Q_{st} (C ₂ H ₂) (kJ/mol)	Q_{st} (CO ₂) (kJ/mol)	IAST selectivity	C ₂ H ₂ /CO ₂ uptake ratio	CCDC codes	CSD Refcodes	Ref
C ₂ H ₂ /CO ₂ adsorption by thermodynamic mechanism									
CAU-10-H	89.8	60	27	25	4	1.5	1454067	OQOCAA	[1]
Cu ^I @UiO-66-(COOH) ₂	51.7	20	74.5	28.9	73*	2.58	N.A.	N.A.	[2]
JCM-1	75	38	36.9	33.4	13.7	1.97	1588763	DIGYIE	[3]
NKMOF-1-Ni	61	51.1	60.3	40.9	26	1.19	1827361	WIHQEM	[4]
FJU-90	180	103	25.1	20.7	4.3	1.75	1882901	RIVSIB	[5]
MAF-2	70.1	19.04	29.8	25.8	N.A.	3.68	2156893	BOGXIF	[7]
NTU-66-Cu	111.5	49	32.3	21.7	6	2.27	1949670	MOVTOJ	[8]
iMOF-5C	32.48	14.56	35.5	N.A.	6	2.23	2058422	LAMYIL	[9]
iMOF-6C	24.86	13.22	38	N.A.	8	1.17	N.A.	N.A.	[9]
iMOF-7C	15.68	13.66	35	N.A.	4	1.15	N.A.	N.A.	[9]
MIL-160	190.85	90.05	31.8	26.9	10	2.12	1828695	PIBZUY	[10]
CAU-23	118.9	71.9	26.7	20	3.8	1.65	1979247	SUFVOH	[10]
ZJU-60	150	73.9	17.6	15.2	N.A.	2.05	969710	ZISNEW	[11]
UTSA-68a	70.1	39.6	25.8	26	3.4 ^a	1.77	1442921	NAFSOF	[12]
JXNU-5a	55.9	34.8	32.9	25.2	5	1.61	1891457	HOFWUX	[13]
FeNi-M' MOF	96	60.9	27	24.5	24	1.58	1958795	LUFRIO01	[14]
SNNU-150-In	153.2	56	23.4	24.9	7	1.51	1923021	LUJRUG	[15]
SNNU-150-Al	97	44.4	29	24	7.27	2.18	N.A.	N.A.	[15]
FJU-36a	52.2	35.5	32.9	31.1	2.8	1.47	1856695	GINDAL	[16]
Cu(BDC-Br)	34.3	24.2	26.1	25.6	3.9	1.42	1936264	FOVDAY	[17]
TCuI	49.3	35.8	38.4	30.7	5.3	1.375	N.A.	N.A.	[18]
TCuCl	67.2	44.8	41	30.1	16.9	1.5	1961542	GUKNOS	[18]
TCuBr	62.7	44.8	36.8	26.8	9.5	1.4	1961541	GUKNIM	[18]

SNNU-45	133.9	97.44	39.9	27.1	8.5	1.37	N.A.	N.A.	[19]
SNNU-63	91.1	43.7	21.6	21.9	2.7	2.08	1947655	KUTDEL	[20]
SNNU-65-Cu-Sc	178.9	70.4	44.9	22.2	13.5	2.5	N.A.	N.A.	[21]
SNNU-65-Cu-Fe	162.3	64.9	28.2	21.8	6.7	2.5	N.A.	N.A.	[21]
SNNU-65-Cu-Ga	141.6	58.7	31.7	20.5	18.7	2.4	1542966	DENLUG	[21]
SUUN-In	153.3	56.1	23.4	24.9	7	2.7	N.A.	N.A.	[21]
ZJU-74a	85.7	69	44.5	30	36.5	1.25	1970545	DUMFID	[22]
ATC-Cu	112.2	90.05	79.1	N.A.	53.6	1.25	2052339	IMAYUT	[23]
JNU-1	61.6	50.4	13	24	3	1.2	1890470	FIWYUI	[24]
MUF-17	67.4 ^b	56.2 ^b	49.5	33.8	6 ^b	1.2	1907595	WOJVAV	[25]
PCM-48	25.54	21.73	26.3	15.4	4.3	1.175	1846945	SIQCED	[26]
SIFSIX-Cu-TPA	185.2	107.3	39.1	25.7	5.2	1.06	2038309	EMOWAH	[27]
UTSA-74a	107	71	31.7	25	9	1.5	1046718	OLEYAH	[28]
PCP-33	121.8	58.6	27.5	26.2	6	2.08	1030846	IGULIH	[29]
NTU-55	135.5	70	25	22	4	1.94	1945415	SUKTIE	[30]
ZJU-199	128	62.4	38.5	19	4 ^a	2.05	1457428	AYOQEM	[31]
UPC-200(Al)-F-B IM	144.5	55.5	20.5	14.2	3.15	2.6	1965168	QUDXUL	[32]
ZJU-195a	214.2	105	29.9	20.7	4.7	2.04	1533108	WAQKUX	[33]
ZJNU-13	118.4	87.9	33.5	22.5	5.64	1.35	1960058	N.A.	[34]
DICRO-4--Ni-i	43	23	37.7	33.9	13.9	1.87	1519267	XIKTAP	[35]
Ni ₃ (HCOO) ₆	94	68	40.9	24.5	22	1.38	N.A.	N.A.	[36]
ZJUT-2	76 ^a	49 ^a	41.5	31.5	10 ^a	1.55	N.A.	N.A.	[37]
SIFSIX-21-Ni	90	29.1	37.9	19.8	27.7	3.1	2052047	EZOTOF	[38]
sql-16-Cu-NO ₃	34.7	16.7	38.6	25.6	78	2.1	2033388	BANHAD	[39]
FJU-22a	114.8	111.3	23	N.A.	N.A.	1.03	1421054	OLUHAG	[40]
SIFSIX-17-Ni	74	51.5	44.2	40.2	11.7	1.44	N.A.	N.A.	[41]
TIFSIX-17-Ni	73	47	48.3	37.8	20.9	1.55	2050185	UQAVAW	[41]
IPM-101	57.1	68.1	43.7	30.7	5.4	0.84	2054903	N.A.	[42]

BSF-1	52.5	39.7	30.7	21.7	3.4	1.32	1893148	RODMIJ	[43]
BSF-2	41.5	29.7	37.3	28.7	5.1	1.4	1952112	VUDBII	[44]
BSF-3	81.7	47.3	42.7	25.5	16.3	1.73	1956266	FUVFAG	[45]
BSF-3-Co	86.2	54	N.A.	N.A.	12.7	1.67	N.A.	N.A.	[45]
BSF-4	53.2	35.8	35.0	24.5	9.8	1.5	1979961	MUMNAM	[46]
BSF-9(ZNU-1)	76.3	38.1	54.0	44.0	56.6	2.0	2090044	N.A.	[47]
BSF-10	65	25.8	34.8	22.9	5.86	2.52	2168393/ 2168394	N.A.	This work
C₂H₂/CO₂ adsorption by molecular sieving mechanism									
UTSA-300	68.9	3.36	57.6	N.A.	743	20.5	1542453	SAXPAL	[48]
ZNU-3	81	5.44	23.4	N.A.	N.A.	14.9	2127132	N.A.	[49]
SIFSIX-dps-Cu	102.3	13.66	60.5	N.A.	1786.6	7.5	N.A.	N.A.	[50]
GeFSIX-dps-Cu	90.5	10.08	56.3	N.A.	171.9	8.98	2060207	FAWXOU	[50]
NTU-65	75.26	2.24	N.A.	N.A.	N.A.	33.6	1961037	QULPUL03	[51]
CPL-1-NH ₂	41.2	4.7	50	32.4	119	8.76	2099886	UZAQIY	[52]
[a] At 296 K. [b] At 293 K									
N.A. = not available.									
* The reported value of 185 in Ref 24 is a mistake. 185 is the IAST selectivity under 273 K (see Figure S29 in Ref. 24) while the IAST selectivity for C ₂ H ₂ /CO ₂ (1/1) at 298 K is ~73.									

- [1] J. Pei, H. Wen, X. Gu, Q. Qian, Y. Yang, Y. Cui, B. Li, B. Chen and G. Qian, Dense Packing of Acetylene in a Stable and Low-Cost Metal-Organic Framework for Efficient C₂H₂/CO₂ Separation, *Angew. Chem. Int. Ed.* 2021, **60**, 25068-25074.
- [2] L. Zhang, K. Jiang, L. Yang, L. Li, E. Hu, L. Yang, K. Shao, H. Xing, Y. Cui, Y. Yang, B. Li, B. Chen and G. Qian, Benchmark C₂H₂/CO₂ Separation in an Ultra-Microporous Metal-Organic Framework via Copper(I)-Alkynyl Chemistry, *Angew. Chem. Int. Ed.* 2021, **60**, 15995-16002.
- [3] J. Lee, C. Y. Chuah, J. Kim, Y. Kim, N. Ko, Y. Seo, K. Kim, T. H. Bae and E. Lee, Separation of Acetylene from Carbon Dioxide and Ethylene by a Water-Stable Microporous Metal-Organic Framework with Aligned Imidazolium Groups inside the Channels, *Angew.*

Chem. Int. Ed., 2018, **57**, 7869-7873.

- [4] Y. Peng, T. Pham, P. Li, T. Wang, Y. Chen, K. Chen, K. Forrest, B. Space, P. Cheng, M. Zaworotko and Z. Zhang, Robust Ultramicroporous Metal-Organic Frameworks with Benchmark Affinity for Acetylene, *Angew. Chem., Int. Ed.*, 2018, **57**, 10971-10975.
- [5] Y. Ye, Z. Ma, R. Lin, R. Krishna, W. Zhou, Q. Lin, Z. Zhang, S. Xiang and B. Chen, Pore Space Partition within a Metal-Organic Framework for Highly Efficient C₂H₂/CO₂ Separation, *J. Am. Chem. Soc.*, 2019, **141**, 4130-4136.
- [6] P. Li, Y. He, Y. Zhao, L. Weng, H. Wang, R. Krishna, H. Wu, W. Zhou, Y. Han and B. Chen, A Rod-Packing Microporous Hydrogen-Bonded Organic Framework for Highly Selective Separation of C₂H₂/CO₂ at Room Temperature. *Angew. Chem. Int. Ed.*, 2015, **127**, 584-587.
- [7] J. Zhang and X. Chen, Optimized Acetylene/Carbon Dioxide Sorption in a Dynamic Porous Crystal, *J. Am. Chem. Soc.*, 2019, **131**, 5516-5521.
- [8] S. Chen, N. Behera, C. Yang, Q. Dong, B. Zheng, Y. Li, Q. Tang, Z. Wang, Y. Wang and J. Duan, A chemically stable nanoporous coordination polymer with fixed and free Cu²⁺ ions for boosted C₂H₂/CO₂ separation, *Nano Res.*, 2020, **14**, 546-553.
- [9] S. Dutta, S. Mukherjee, O. T. Qazvini, A. K. Gupta, S. Sharma, D. Mahato, R. Babarao and S. K. Ghosh, Three-in-One C₂H₂-Selectivity-Guided Adsorptive Separation across an Isoreticular Family of Cationic Square-Lattice MOFs, *Angew. Chem. Int. Ed.* 2022, **61**, e202114132.
- [10] Y. Ye, S. Xian, H. Cui, K. Tan, L. Gong, B. Liang, T. Pham, H. Pandey, R. Krishna, P. Lan, K. Forrest, B. Space, T. Thonhauser, J. Li and S. Ma, Metal-Organic Framework Based Hydrogen-Bonding Nanotrap for Efficient Acetylene Storage and Separation, *J. Am. Chem. Soc.* 2022, **144**, 1681-1689.
- [11] X. Duan, Q. Zhang, J. Cai, Y. Yang, Y. Cui, Y. He, C. Wu, R. Krishna, L. Chen and G. Qian, A new metal-organic framework with potential for adsorptive separation of methane from carbon dioxide, acetylene, ethylene, and ethane established by simulated breakthrough experiments, *J. Mater. Chem. A*, 2014, **2**, 2628-2633.
- [12] G. Chang, B. Li, H. Wang, T. Hu, Z. Bao and B. Chen, Control of interpenetration in a microporous metal-organic framework for significantly enhanced C₂H₂/CO₂ separation at

- room temperature, *Chem. Commun.*, 2016, **52**, 3494-3496.
- [13] R. Liu, Q. Liu, R. Krishna, W. Wang, C. He and Y. Wang, Water-Stable Europium 1,3,6,8-Tetrakis(4-carboxylphenyl)pyrene Framework for Efficient C₂H₂/CO₂ Separation, *Inorg. Chem.*, 2019, **58**, 5089-5095.
- [14] J. Gao, X. Qian, R. Lin, R. Krishna, H. Wu, W. Zhou and B. Chen, Mixed Metal-Organic Framework with Multiple Binding Sites for Efficient C₂H₂/CO₂ Separation, *Angew. Chem. Int. Ed*, 2020, **59**, 4396-4400.
- [15] H. Lv, Y. Li, Y. Xue, Y. Jiang, S. Li, M. Hu and Q. Zhai, Systematic Regulation of C₂H₂/CO₂ Separation by 3p-Block Open Metal Sites in a Robust Metal-Organic Framework Platform, *Inorg. Chem.* 2020, **59**, 4825-4834.
- [16] L. Z. Liu, Z. Z. Yao, Y. X. Ye, L. J. Chen, Q. J. Lin, Y. S. Yang, Z. J. Zhang, S. C. Xiang and J. Robustness, Selective Gas Separation, and Nitrobenzene Sensing on Two Isomers of Cadmium Metal-Organic Frameworks Containing Various Metal-O-Metal Chains, *Inorg. Chem.*, 2018, **57**, 12961–12968.
- [17] H. Cui, Y. X. Ye, H. Arman, Z. Q. Li, A. Alsalme, R. B. Lin and L. Chen, Microporous Copper Isophthalate Framework of mot Topology for C₂H₂/CO₂ Separation, *Cryst. Growth Des.*, 2019, **19**, 5829–5835.
- [18] S. Mukherjee, Y. He, D. Franz, S. Q. Wang, W. R. Xian, A. A. Bezrukov, B. Space, Z. Xu, J. He and M. J. Zaworotko, Halogen-C₂H₂ Binding in Ultramicroporous Metal-Organic Frameworks (MOFs) for Benchmark C₂H₂/CO₂ Separation Selectivity, *Chem.-Eur. J.*, 2020, **26**, 4923–4929.
- [19] Y. Li, Y. Wang, Y. Xue, H. Li, Q. Zhai, S. Li, Y. Jiang, M. Hu and X. Bu, Ultramicroporous Building Units as a Path to Bi-microporous Metal-Organic Frameworks with High Acetylene Storage and Separation Performance, *Angew. Chem. Int. Ed.* 2019, **58**, 13590-13595.
- [20] Y. T. Li, J. W. Zhang, H. J. Lv, M. C. Hu, S. N. Li, Y. C. Jiang and Q. G. Zhai, Tailoring the Pore Environment of a Robust Ga-MOF by Deformed [Ga₃O(COO)₆] Cluster for Boosting C₂H₂ Uptake and Separation, *Inorg. Chem.*, 2020, **59**, 10368 – 10373.
- [21] J. W. Zhang, M. C. Hu, S. N. Li, Y. C. Jiang, P. Qu and Q. G. Zhai, Assembly of [Cu₂(COO)₄] and [M₃(μ₃-O)(COO)₆] (M = Sc, Fe, Ga, and In) building blocks into porous

frameworks towards ultra-high C₂H₂/CO₂ and C₂H₂/CH₄ separation performance, *Chem. Commun.*, 2018, **54**, 2012-2015.

- [22] J. Pei, K. Shao, J. X. Wang, H.-M. Wen, Y. Yang, Y. Cui, R. Krishna, B. Li and G. D. Qian, A Chemically Stable Hofmann-Type Metal–Organic Framework with Sandwich-Like Binding Sites for Benchmark Acetylene Capture, *Adv. Mater.*, 2020, **32**, 1908275.
- [23] Z. Niu, X. Cui, T. Pham, G. Verma, P. C. Lan, C. Shan, H. Xing, K. A. Forrest, S. Suepaul, B. Space, A. Nafady, A. M. Al-Enizi and S. Ma, A MOF-based Ultra-Strong Acetylene Nano-trap for Highly Efficient C₂H₂/CO₂ Separation, *Angew. Chem. Int. Ed.* 2021, **60**, 5283-5288.
- [24] H. Zeng, M. Xie, Y. L. Huang, Y. F. Zhao, X. J. Xie, J. P. Bai, M. Y. Wan, R. Krishna, W. G. Lu and D. Li, Induced Fit of C₂H₂ in a Flexible MOF Through Cooperative Action of Open Metal Sites, *Angew. Chem. Int. Ed.*, 2019, **58**, 8515-8519.
- [25] O. T. Qazvini, R. Babarao and S. G. Telfer, Multipurpose Metal-Organic Framework for the Adsorption of Acetylene: Ethylene Purification and Carbon Dioxide Removal, *Chem. Mater.*, 2019, **31**, 4919-4926.
- [26] J. Reynoids, K. Walsh, B. Li, P. Kunal, B. Chen and S. Humphrey, Highly selective room temperature acetylene sorption by an unusual triacetylenic phosphine MOF, *Chem. Commun.*, 2018, **54**, 9937-9940.
- [27] H. Li, C. Liu, C. Chen, Z. Di, D. Yuan, J. Pang, W. Wei, M. Wu and M. Hong, An Unprecedented Pillar-Cage Fluorinated Hybrid Porous Framework with Highly Efficient Acetylene Storage and Separation, *Angew. Chem. Int. Ed.* 2021, **60**, 7547.
- [28] F. Luo, C. S. Yan, L. L. Dang, R. Krishna, W. Zhou, H. Wu, X. L. Dong, Y. Han, T. L. Hu, M. O’Keeffe, L. L. Wang, M. B. Luo, R. B. Lin and L. Chen, UTSA-74: A MOF-74 Isomer with Two Accessible Binding Sites per Metal Center for Highly Selective Gas Separation, *J. Am. Chem. Soc.*, 2016, **138**, 5678-5684.
- [29] J. G. Duan, W. Q. Jin and R. Krishna, Natural Gas Purification Using a Porous Coordination Polymer with Water and Chemical Stability, *Inorg. Chem.*, 2015, **54**, 4279-4284.
- [30] Q. B. Dong, Y. N. Guo, H. F. Cao, S. N. Wang, R. Matsuda and J. G. Duan, Accelerated C₂H₂/CO₂ Separation by a Se-Functionalized Porous Coordination Polymer with Low Binding Energy, *ACS Appl. Mater. Interfaces*, 2020, **12**, 3764-3772.

- [31] L. Zhang, C. Zou, M. Zhao, K. Jiang, R. B. Lin, Y. B. He, C. D. Wu, Y. J. Cui, B. Chen and G. D. Qian, Doubly Interpenetrated Metal-Organic Framework for Highly Selective C₂H₂/CH₄ and C₂H₂/CO₂ Separation at Room Temperature, *Cryst. Growth Des.*, 2016, **16**, 7194-7197.
- [32] W. D. Fan, S. Yuan, W. J. Wang, L. Feng, X. P. Liu, X. R. Zhang, X. Wang, Z. X. Kang, F. N. Dai, D. Q. Yuan, D. F. Sun and H. C. Zhou, Optimizing Multivariate Metal-Organic Frameworks for Efficient C₂H₂/CO₂ Separation, *J. Am. Chem. Soc.*, 2020, **142**, 8728-8737.
- [33] L. Zhang, K. Jiang, Y. Li, D. Zhao, Y. Yang, Y. Cui, B. Chen and G. Qian, Microporous Metal-Organic Framework with Exposed Amino Functional Group for High Acetylene Storage and Excellent C₂H₂/CO₂ and C₂H₂/CH₄ Separations, *Cryst. Growth Des.*, 2017, **17**, 2319-2322.
- [34] T. Xu, Z. Jiang, P. Liu, H. Chen, X. Lan, D. Chen, L. Li and Y. He, Immobilization of Oxygen Atoms in the Pores of Microporous Metal-Organic Frameworks for C₂H₂ Separation and Purification, *ACS Appl. Nano Mater.*, 2020, **3**, 2911-2919.
- [35] H. S. Scott, M. Shivanna, A. Bajpai, D. G. Madden, K. J. Chen, T. Pham, K. A. Forrest, A. Hogan, B. Space, J. J. Perry and M. J. Zaworotko, Highly Selective Separation of C₂H₂ from CO₂ by a New Dichromate-Based Hybrid Ultramicroporous Material, *ACS Appl. Mater. Interfaces*, 2017, **9**, 33395-33400.
- [36] L. Zhang, K. Jiang, J. Zhang, J. Pei, K. Shao, Y. Cui, Y. Yang, B. Li, B. Chen and G. D. Qian, Low-Cost and High-Performance Microporous Metal-Organic Framework for Separation of Acetylene from Carbon Dioxide, *ACS Sustainable Chem. Eng.* 2019, **7**, 1667-1672.
- [37] H. Wen, C. Liao, L. Li, L. Yang, J. Wang, L. Huang, B. Li, B. Chen and J. Hu, Reversing C₂H₂-CO₂ adsorption selectivity in an ultramicroporous metal-organic framework platform, *Chem. Commun.*, 2019, **55**, 11354-11357.
- [38] N. Kumar, S. Mukherjee, N. C. Harvey-Reid, A. A. Bezrukov, K. Tan, V. Martins, M. Vandichel, T. Pham, P. E. Kruger and M. J. Zaworotko, Breaking the trade-off between selectivity and adsorption capacity for gas separation, *Chem.* 2021, **7**, 3085-3098.
- [39] N. Kumar, S. Mukherjee, A. Bezrukov, M. Vandichel, M. Shivanna, D. Sensharma, A. Bajpai, V. Gascon, K. Otake, S. Kitagawa, M. J. Zaworotko, A square lattice topology

coordination network that exhibits highly selective C₂H₂/CO₂ separation performance, *SmartMat*, 2020, **1**, e1008.

- [40] Z. Yao, Z. Zhang, L. Liu, Z. Liu, W. Zhou, Y. Zhao, Y. Han, B. Chen, R. Krishna and S. Xiang, Extraordinary Separation of Acetylene-Containing Mixtures with Microporous Metal-Organic Frameworks with Open O Donor Sites and Tunable Robustness through Control of the Helical Chain Secondary Building Units, *Chem.Eur.J*, 2016, **22**, 5676-5683.
- [41] S. Mukherjee, N. Kumar, A. A. Bezrukov, K. Tan, T. Pham, K. a. Forrest, K. A. Oyekan, O. T. Qazvini, D. G. Madden, B. Space and M. J. Zaworotko, Amino-Functionalised Hybrid Ultramicroporous Materials that Enable Single-Step Ethylene Purification from a Ternary Mixture, *Angew. Chem. Int. Ed*, 2021, **60**, 10902-10909.
- [42] S. Sharma, S. Mukherjee, A. V. Desai, M. Vandichel, G. K. Dam, A. Jadhav, G. Kociok-Kohn, M. J. Zaworotko and S. K. Ghosh, Efficient Capture of Trace Acetylene by an Ultramicroporous Metal-Organic Framework with Purine Binding Sites, *Chem. Mater.*, 2021, **33**, 5800-5808.
- [43] Y. Zhang, L. Yang, L. Wang, S. Duttwyler and H. Xing, A Microporous Metal-Organic Framework Supramolecularly Assembled from a Cu^{II} Dodecaborate Cluster Complex for Selective Gas Separation, *Angew. Chem. Int. Ed.* 2019, **58**, 8145-8150.
- [44] Y. Zhang, L. Yang, L. Wang and H. Xing, Pillar iodination in functional boron cage hybrid supramolecular frameworks for high performance separation of light hydrocarbons, *J. Mater. Chem. A*, 2019, **7**, 27560-27566.
- [45] Y. Zhang, J. Hu, R. Krishna, L. Wang, L. Yang, X. Cui, S. Duttwyler and H. Xing, Rational Design of Microporous MOFs with Anionic Boron Cluster Functionality and Cooperative Dihydrogen Binding Sites for Highly Selective Capture of Acetylene, *Angew. Chem. Int. Ed.*, 2020, **59**, 17664-17669.
- [46] Y. Zhang, L. Wang, J. Hu, S. Duttwyler, X. Cui and H. Xing, Solvent-dependent supramolecular self-assembly of boron cage pillared metal-organic frameworks for selective gas separation, *CrystEngComm*, 2020, **22**, 2649-2655.
- [47] L. Wang, W. Sun, Y. Zhang, N. Xu, R. Krishna, J. Hu, Y. Jiang, Y. He and H. Xing, Interpenetration Symmetry Control Within Ultramicroporous Robust Boron Cluster Hybrid MOFs for Benchmark Purification of Acetylene from Carbon Dioxide, *Angew. Chem. Int. Ed.*

2021, **60**, 22865-22870.

- [48] R. Lin, L. Li, H. Wu, H. Arman, B. Li, R. G. Lin, W. Zhou and B. Chen, Optimized Separation of Acetylene from Carbon Dioxide and Ethylene in a Microporous Material, *J. Am. Chem. Soc.*, 2017, **139**, 8022-8028.
- [49] W. Sun, J. Hu, Y. Jiang, N. Xu, L. Wang, J. Li, Y. Hu, S. Duttwyler and Y. Zhang, Flexible molecular sieving of C₂H₂ from CO₂ by a new cost-effective metal organic framework with intrinsic hydrogen bonds, *Chem. Eng. J.*, 2022, **439**, 135745.
- [50] J. Wang, Y. Zhang, Y. Su, X. Liu, P. Zhang, R. Lin, S. Chen, Q. Deng, Z. Zeng, S. Deng and B. Chen, Fine pore engineering in a series of isoreticular metal-organic frameworks for efficient C₂H₂/CO₂ separation, *Nat Commun.*, 2022, **13**, 200.
- [51] Q. Dong, X. Zhang, S. Liu, R. Lin, Y. Guo, Y. Ma, A. Yonezu, R. Krishna, G. Liu, J. Duan, R. Matsuda, W. Jin and B. Chen, Tuning Gate-Opening of a Flexible Metal-Organic Framework for Ternary Gas Sieving Separation, *Angew. Chem. Int. Ed.* 2020, **59**, 22756-22762.
- [52] L. Yang, L. Yan, Y. Wang, Z. Liu, J. He, Q. Fu, D. Fu, D. Liu, X. Gu, P. Dai, L. Li and X. Zhao, Adsorption Site Selective Occupation Strategy within a Metal-Organic Framework for Highly Efficient Sieving Acetylene from Carbon Dioxide, *Angew. Chem. Int. Ed.*, 2021, **60**, 4570-4574.